metals

MDPI

Article

Depression of Pyrite in Seawater Flotation by Guar Gum

César I. Castellón [1], Eder C. Piceros [2], Norman Toro [3,4], Pedro Robles [5], Alejandro López-Valdivieso [6] and Ricardo I. Jeldres [1,*]

1 Departamento de Ingeniería Química y Procesos de Minerales, Facultad de Ingeniería, Universidad de Antofagasta, Av. Angamos 601, Antofagasta 1240000, Chile; castelloniv@gmail.com
2 Faculty of Engineering and Architecture, Universidad Arturo Prat, PO Box 121, Iquique 1100000, Chile; edpicero@unap.cl
3 Departamento de Ingeniería Metalúrgica y Minas, Universidad Católica del Norte, Antofagasta 1270709, Chile; ntoro@ucn.cl
4 Department of Mining, Geological and Cartographic Department, Universidad Politécnica de Cartagena, 30202 Murcia, Spain
5 Escuela de Ingeniería Química, Pontificia Universidad Católica de Valparaíso, Valparaíso 2340000, Chile; pedro.robles@pucv.cl
6 Instituto de Metalurgia, Laboratorio de Química de Superficies, Universidad Autónoma de San Luis Potosí, Av. Sierra Leona 550, San Luis Potosi 78210, México; alopez@uaslp.mx
* Correspondence: ricardo.jeldres@uantof.cl; Tel.: +56-552-637-901

Received: 21 January 2020; Accepted: 7 February 2020; Published: 11 February 2020

Abstract: The application of guar gum for pyrite depression in seawater flotation was assessed through microflotation tests, Focused Beam Reflectance Measurements (FBRM), and Particle Vision Measurements (PVM). Potassium amyl xanthate (PAX) and methyl isobutyl carbinol (MIBC) were used as collector and frother, respectively. Chemical species on the pyrite surface were characterized by Fourier-transform infrared spectroscopy (FTIR) spectroscopy. The microflotation tests were performed at pH 8, which is the pH at the copper sulfide processing plants that operate with seawater. Pyrite flotation recovery was correlated with FBRM and PVM characterization to delineate the pyrite depression mechanisms by the guar gum. The high flotation recovery of pyrite with PAX was significantly lowered by guar gum, indicating that this polysaccharide could be used as an effective depressant in flotation with sea water. FTIR analysis showed that PAX and guar gum co-adsorbed on the pyrite surface, but the highly hydrophilic nature of the guar gum embedded the hydrophobicity due to the PAX. FBRM and PVM revealed that the guar gum promoted the formation of flocs whose size depended on the addition of guar gum and PAX. It is proposed that the highest pyrite depression occurred not only because of the hydrophilicity induced by the guar gum, but also due to the formation of large flocs, which could not be transported by the bubbles to the froth phase. Furthermore, it is shown that an overdose of guar gum hindered the depression effect due to redispersion of the flocs.

Keywords: seawater flotation; pyrite depression; guar gum; FBRM

1. Introduction

Pyrite is the most abundant iron sulfide mineral, and it is commonly associated as a gangue with ores of base metals such as chalcopyrite, galena, sphalerite, etc. Its presence can be involved in operational terms since it tends to float, even in some instances without the use of collectors [1,2]. Interestingly, it is simple to manage physicochemical changes in its surface, which can lead to significant consequences in its floatability, for example, it has been widely exhibited that the recovery of the

pyrite declines by rising the pH [3–5]. This inverse relationship between recovery and pH has been associated with the greater abundance of hydrophilic hydroxides concerning hydrophobic sulfides that found on the pyrite surface. This happens because, at alkaline conditions, ferric hydroxide is generated from the ferrous hydroxide released from inside the pyrite [6–8]. Subsequently, ferric hydroxide that has a hydrophilic nature precipitates on the surface of the pyrite, decreasing its contact angle and consequently lowering its floatability [9,10]. In this way, by regulating the pH with alkalizing agents such as sodium hydroxide, sodium carbonate, or lime, it can make the pyrite no float. An interesting aspect is that lime is more effective compared to sodium hydroxide, which is explained by the participation of calcium ions as, at pH less than 12.5, $Ca(OH)^+$ is the main component of the solution. This hydrophilic element has a high affinity for the surface of pyrite, so it also helps to boost their depression. It is common that in the copper industry lime is used as the sole depressant for pyrite, primarily when flotation is carried out in freshwater [11,12]. Interestingly, the use of seawater is a strategy that is being frequently adopted in sectors that have a shortage of freshwater, highlighting mining plants in countries such as Chile, Australia, Indonesia, etc. [13]. However, when the operations are carried out in seawater, these are unlikely to operate under highly alkaline conditions, mainly for two reasons: (i) the buffer effect of seawater implies that the lime consumption required to reach pH 11 is about ten times higher than in freshwater [14,15]. This excessive addition of lime means a considerable extra cost to the process, in addition to an increase of water hardness. (ii) Calcium and magnesium ions precipitate, which significantly affects the recovery of molybdenite and copper sulfides [16–19]. For these reasons, one of the main recommendations is working at a natural pH (or close to it), separating pyrite through the addition of new depressants reagents. Commercially, cyanide has been used for pyrite depression in several plants; however, due to its toxicity and the associated environmental concerns, further reagents are demanded, including sulfur dioxide, sodium sulfite, or metabisulphite of sodium. Many studies have shown that these reagents suppress xanthate adsorption by reducing the mixed potential to levels below the potential required for the oxidation of xanthate to dixanthogen [20–23]. The dixanthogen is a hydrophobic molecule generated from xanthate. Its presence is one of the leading causes by which pyrite increases its hydrophobicity, but the sulfoxide reagents may favor the formation of hydroxide species on the surface of pyrite; although, in most cases, these reagents do not achieve expected performances, and even environmental problems might arise that in some instances make impossible its implementation. Alternatively, many researchers have attempted to incorporate organic reagents into the processes, which have frequently shown their ability to selectively adsorb on the surface of pyrite, avoiding the collector adsorption and assigning some level of hydrophilicity [24–28]. The structure of these reagents is composed of (i) a hydrocarbon chain; (ii) hydroxyl groups that are distributed through the polymer structure, which are capable of ionizing or forming hydrogen bonds; and (iii) strongly hydrated polar groups such as SO_3^{-2}, COO^-, etc., which are also dispersed throughout the molecule. The biopolymers can be adsorbed to the surface of the pyrite by assigning a higher hydrophilic character to the surface, reducing the chances of adhesion between the particle and the bubble. Mu et al. [29] stated that four mechanisms for the adsorption of biopolymers should be considered: (i) electrochemical attraction, (ii) hydrophobic interaction, (iii) hydrogen bonds, and (iv) chemical interaction. Lopez-Valdivieso et al. [30] pointed that the oxidation state of the pyrite is one of the most relevant aspects for the adsorption of biopolymers like dextrin, wherein the amount of adsorbed molecules was directly correlated to the surface density of ferric hydroxide.

Guar gum, defined as an organic polysaccharide, is a galactomannan. Galactomannans have proven to be more effective depressants than starch, dextrin, and carboxymethyl cellulose (CMC). This has been attributed to the stronger hydrogen bonds formed by the cis-hydroxyl pair of long and linear molecules over a large surface area of particles, causing their agglomeration. Therefore, more effective separation of sulfide ore from gangue minerals has been found in froth flotation using guar gum as a depressant [31,32]. Guar gum applications include hindering the flotation of varied minerals such as talc, potash, chromite [33–36], even promising results have been shown to depress pyrite. However, these studies have been limited to the use of freshwater [37]. In this context,

the present research addresses the consequences of using guar gum on pyrite depression in seawater flotation. The assays are carried out at pH 8 to emulate the typical conditions practiced in copper mining plants that use this type of water in their concentration stages. A microscopic analysis seeks to describe the mechanisms involved during the application of this polysaccharide. For this, the properties of pyrite aggregate are directly characterized by the use of the Focused Beam Reflectance Measurement (FBRM) and Particle Vision Measurement (PVM) techniques.

2. Methodology

2.1. Materials

The natural high purity pyrite specimens used in this investigation were acquired from Ward Scientific Establishment Inc. Scanning electron microscopy (SEM), as well as scattered energy x-ray spectroscopy (EDS) are shown in Figure 1 and was used a Zeiss scanning electron microscopy, model EVA MA-10 (CARL ZEISS Ltd., Oberkochen, Germany) and Oxford X-ray detector (OXFORD Instruments, Oxford, UK).

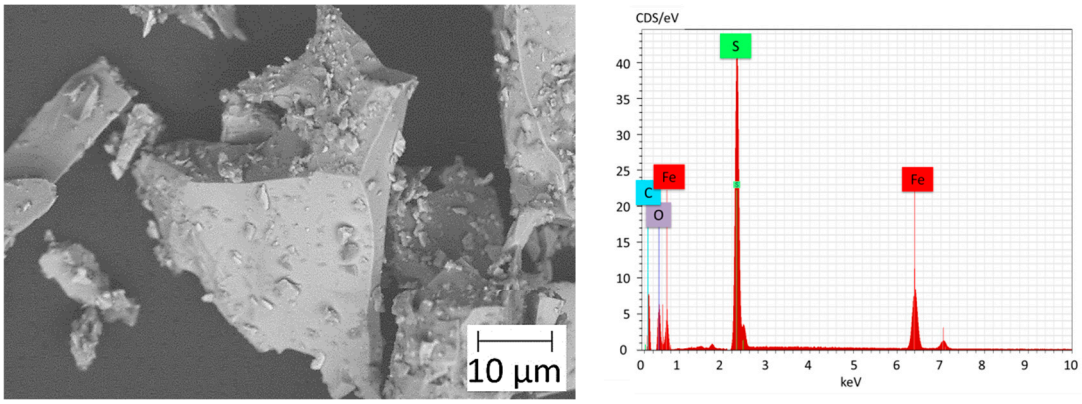

(**A**) (**B**)

Figure 1. (**A**) SEM micrograph of pyrite sample and (**B**) energy x-ray spectroscopy (EDS) spectrum.

Two different sizes of pyrite were prepared, considering a range between 38 and 65 µm (−65 + 38 µm) for micro flotation tests and −38 µm for flocculation kinetics tests. Seawater was obtained 200 m from the coast of San Jorge Bay (Antofagasta, Chile) and it was filtered by UV filter to eliminate bacterial activity. Before being used, seawater passed through a quartz sand filter (50 µm) and a mechanical polyethylene filter (1 µm) to remove insoluble particles. Chemical analysis is presented in Table 1, which were obtained by different analytical techniques (atomic absorption spectrometry (AAS), Argentometric method, and acid–base volumetry).

Table 1. Seawater ion concentration and method of analysis (pH 8).

Ion	Concentration [mg/L]	Method of Analysis
Na^+	9950	Atomic absorption spectrometry
Mg^{2+}	1250	Atomic absorption spectrometry
Ca^{2+}	400	Atomic absorption spectrometry
K^+	380	Atomic absorption spectrometry
Cl^-	19,450	Argentometric method
HCO_3^-	150	Acid–base volumetry

Flotation reagents were potassium amyl xanthate (PAX) as collector and methyl isobutyl carbinol (MIBC) as frother. Commercial xanthates generally have a purity of between 60 and 90%. They usually contain residual alkali hydroxide or metal carbonate that is intentionally added to slow down the

decomposition of the product during storage. Because of this, PAX was purified by dissolving it in acetone and recrystallizing from diethyl ether. All aqueous solutions were prepared using distilled water. Guar gum G4129 of high purity was supplied by Sigma-Aldrich (see the chemical structure in Figure 2).

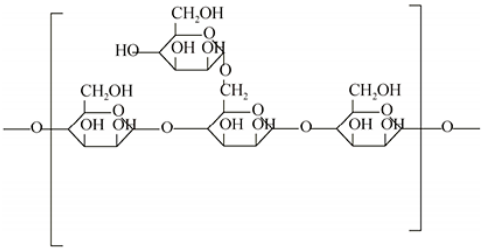

Figure 2. Chemical structure of guar gum.

2.2. Preparation of Flotation Reagents

A stock solution of PAX was prepared by adding 750 mg in a 100 mL flask by filling it up with distilled water. From this solution, the required aliquots were taken to achieve the dosages expected in the tests. For the stock solution of MIBC, 0.021 g of the reagent was added to 100 mL of distilled water. From this, 14.3 mL was taken, which corresponded to a concentration of 20 ppm of MIBC. For the stock solution of guar gum (750 mg/L), the powder was stirred in distilled water for 5 h. From this solution, aliquots were taken to reach the corresponding concentration of guar gum.

2.3. Microflotation Tests

Microflotation tests were carried out in a 150 mL Partridge–Smith glass cell using air at a flowrate of 100 mL/min. Pyrite–water suspensions were prepared using 2 g of pyrite (considering a range between 38 and 65 μm) and 150 mL aqueous solution. The suspensions were stirred in a beaker with magnetic agitation and conditioned at the required pH for 3 min. Afterwards, PAX was added to the suspension at the desired concentration and contacted with the pyrite for 3 min, then with the frothing agent for another 2 min. Finally, the suspension was transferred to a Partridge–Smith cell and flotation was carried out for 3 min, scraping off the froth every 5 s. The pulp level in the microflotation test was kept constant by adding a background solution prepared at the same chemical reagent concentration as the original aqueous solution. To evaluate the influence of the depressant concentration on the floatability of pyrite, guar gum was added before the collector and contacted with the mineral for 5 min. All flotation tests were performed in triplicate. After the microflotation test, the non-floated and floated products were dried and weighed to calculate the pyrite floatability.

2.4. Aggregate Characterization

The effect of reagent conditioning on aggregate characteristics was evaluated; in this case, the mean chord length using the Focused Beam Reflectance Measurement (FBRM) technique. The instrument model was Particle Track G400 with a measurement of every 2 s. Direct images of particle aggregates were obtained with the Particle Vision Measurement (PVM) technique, using the V819 model. Three-hundred milliliters of seawater and 2 grams of pure pyrite were used. After 4 min of mixing, guar gum was added with the desired concentration, and after 5 min, PAX and MIBC were added.

2.5. Fourier Transform Infrared (FTIR) Spectroscopy

FTIR studies were performed to provide information on the infrared spectra of pyrite, PAX, guar gum, and the interaction products between the mineral, the collector, and the polysaccharide. A Fourier Infrared Spectrometer (PerkinElmer, Santiago, Chile) that operates in the range of 4000 to 400 cm^{-1} was used for the spectroscopic studies.

2.6. Surface Tension

Four sets of surface tension tests were performed at pH 8 and 23 °C: (i) seawater, 20 ppm of MIBC and various guar gum concentrations (0–200 ppm); (ii) seawater and various MIBC levels (0–200 ppm); (iii) seawater and various guar gum concentrations (0–200 ppm); and (iv) seawater, 20 ppm of MIBC, 75 ppm of PAX, and various guar gum concentrations (0–200 ppm). The surface tension was determined by the bubble up technique using a tensiometer Lauda model TD 3 (LAUDA DR. R. WOBSER GMBH & CO, Lauda-Königshofen, Germany).

3. Results and Discussions

3.1. Microflotations

Figure 3 presents the recovery of pyrite in seawater as a function of PAX addition in the presence of 20 ppm of MIBC and in the absence of guar gum. The tests were performed at pH 8 to emulate the conditions used in the copper industry that operates with seawater [38]. There is a PAX dosage that maximizes the recovery of pyrite, which was close to 75 ppm. At this PAX addition, the pyrite recovery was 80%. Increasing PAX dosages lead to a little decrease in pyrite recovery.

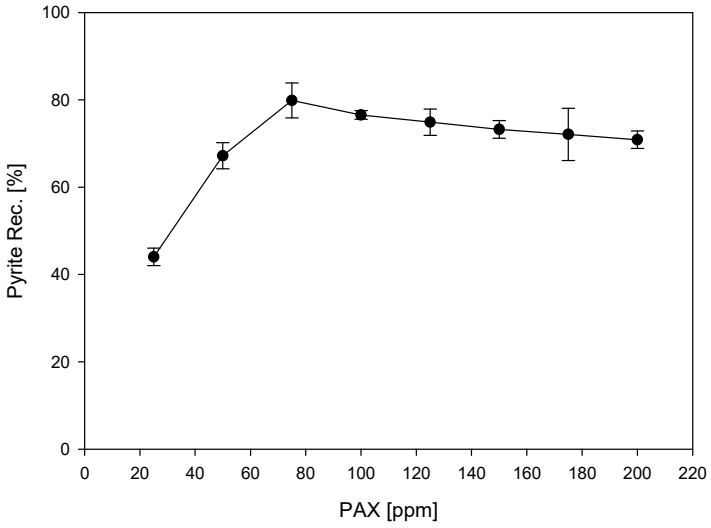

Figure 3. Pyrite recovery as a function of PAX concentration (pH 8, 20 ppm of MIBC).

Dixanthogen formation through the oxidation of the collector ion turns the pyrite surface hydrophobic [39]. This collector oxidation can take place with the reduction of oxygen (Equation (1)). López-Valdivieso et al. [40] proposed that oxidation of the collector ion is coupled with the reduction of surface iron hydroxides (Equation (2)). The pyrite used in this study had iron hydroxides on its surface as will be shown below.

$$ROCS_2^- + \frac{1}{2}O_2 + H_2O \rightarrow (ROCS_2)_2 + 2OH^- \quad (1)$$

$$2ROCS2^- + 2Fe(OH)_3 + 6H^+ = (ROCS2)_2 + 2Fe^{2+} + 6H_2O \quad (2)$$

Figure 4 shows the pyrite flotation recovery as a function of guar gum addition at pH 8 in seawater and in the presence of 75 ppm PAX and 20 ppm MIBC. As the dosage of the polysaccharide increases up to 100 ppm, the recovery of pyrite gradually decreases from 80 to 23%, demonstrating that the polysaccharide is a good pyrite depressant. The OH groups of the guar gum molecules likely adsorbed onto OH sites of ferric hydroxide of the pyrite surface by a similar adsorption mechanism occurring between dextrin and oxidized pyrite [30,41]. The difference between guar gum and dextrin is that two cis-OH groups of the guar gum would link to a ferric hydroxide OH site, whereas, in the case of dextrin,

only one OH group would link to a ferric hydroxide site. As the guar gum is a highly hydrophilic big molecule, its adsorption rendered the pyrite surface very hydrophilic. At guar gum dosages greater than 100 ppm, the recovery of pyrite gradually increased reaching 39% at 200 ppm guar gum.

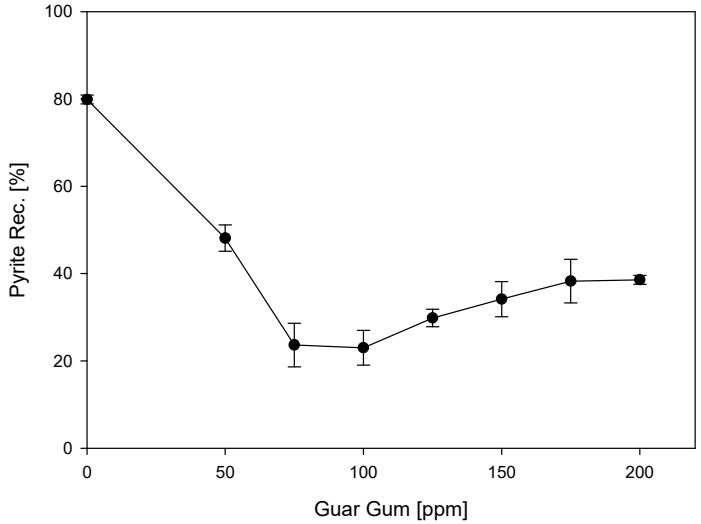

Figure 4. Pyrite recovery as a function of guar gum concentration (pH 8, 75 ppm of PAX, 20 ppm of MIBC).

3.2. *Characterization of Aggregates*

Figures 5–7 present the characterization of pyrite aggregates throughout their chord length (using the FBRM probe), at various concentrations of guar gum without PAX or MIBC. In a collector and frother free environment, guar gum promoted the growth of aggregates, even at low concentrations. Adding 5 ppm polysaccharide, the aggregates grew from 120 to 160 µm (Figure 5A). At the optimal dose (100 ppm), the maximum chord length was slightly higher than 192 µm (Figure 6A). This value is stabilized at further dosages. At 200 ppm guar gum, the maximum aggregate size was 188 µm, suggesting that the limit zone in which the polysaccharide could act as a flocculating agent was reached. A notable difference in all particle flocculation systems is related to the fragmentation of the floc structure, caused by the hydrodynamic conditions. The FBRM probe provides the particle count classified in different bins according to their size, presenting their size evolution over time. In Figure 5B, it can be seen that after the addition of 5 ppm guar gum, the particle count for flocs smaller than 150 microns radically decreased, with a subtle increase of the flocs having a size between 150 and 300 microns. However, within a few seconds of flocculation, the number of flocs (counts) less than 150 microns increased steadily. When the guar gum dosage was 100 ppm, particles smaller than 150 microns are connected to produce larger stable aggregates, indicating that the aggregates are joined with greater strength. Increasing the dosage of guar gum up to 200 ppm raised the particle count again after a few seconds of flocculation (Figure 7A). The excessive amount of polymer may have saturated the particle surface so the polymer bound a less number of particles. Weak aggregates formed at this dosage.

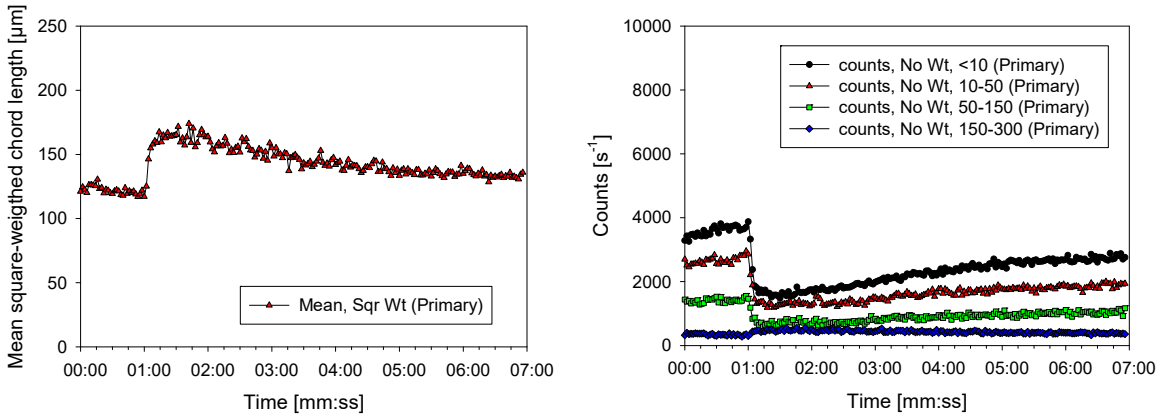

(**A**) (**B**)

Figure 5. (**A**) Mean square chord length and (**B**) counts evolution of suspension; 5 ppm of guar gum added after 1 min (no frother or collector).

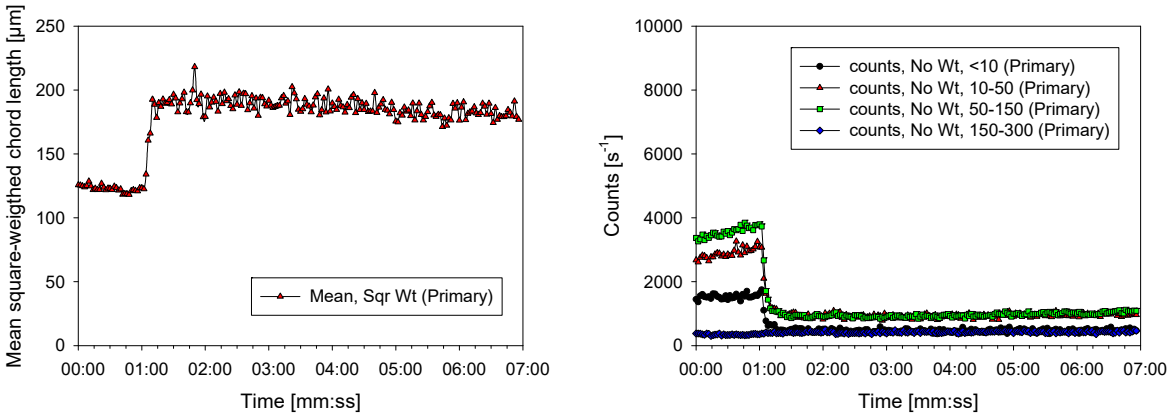

(**A**) (**B**)

Figure 6. (**A**) Mean square chord length and (**B**) counts evolution of suspension; 100 ppm of guar gum added after 1 min (no frother or collector).

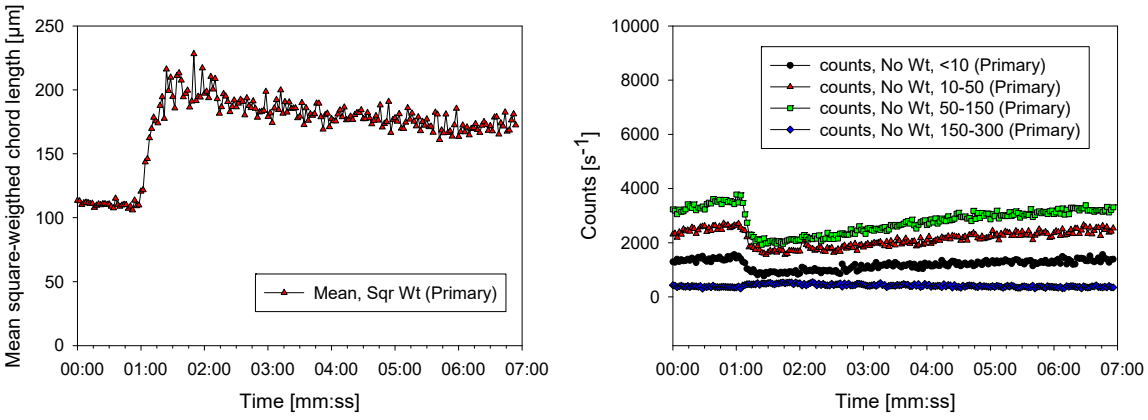

(**A**) (**B**)

Figure 7. (**A**) Mean square chord length and (**B**) counts evolution of suspension; 200 ppm of guar gum added after 1 min (no frother or collector).

Figures 8–10 exhibit the outcomes for the size of the aggregates at different concentrations of guar gum and in the presence of 75 ppm PAX and 20 ppm MIBC. A notable effect of the collector and the frother is the redispersing of the particles that are bound into the floc, especially at low polymer dosages. As shown in Figure 8A, with 5 ppm guar gum, there was an instantaneous growth of aggregates. However, after 1 min, following the addition of PAX and MIBC, a significant dispersion of particles with rope length less than 150 µm was observed. This seems to indicate that guar gum desorbed from the pyrite surface due to xanthate adsorption. Lopez-Valdivieso et al. [30] show that dextrin desorbed from pyrite surface by xanthates. Dispersion of the particles favored the recovery of pyrite since dispersed particles are more prone to float than those that make up an aggregate. According to Figure 8B, the dispersion due to PAX and MIBC is attenuated by increasing the dosage of the polysaccharide. At the optimum pyrite depression concentration of 100 ppm guar gum, the average decrease in aggregates is gradual (Figure 9A). In addition, particles smaller than 150 µm were released in a substantially lower quantity than at low guar gum dosages (Figure 9B) and not significant presence of particles smaller than 10 µm was quantified. Above 100 ppm guar gum, at a 200 ppm guar gum, particles redispersing increased again (Figure 10B), which coincides with the increase in pyrite recovery (Figure 5).

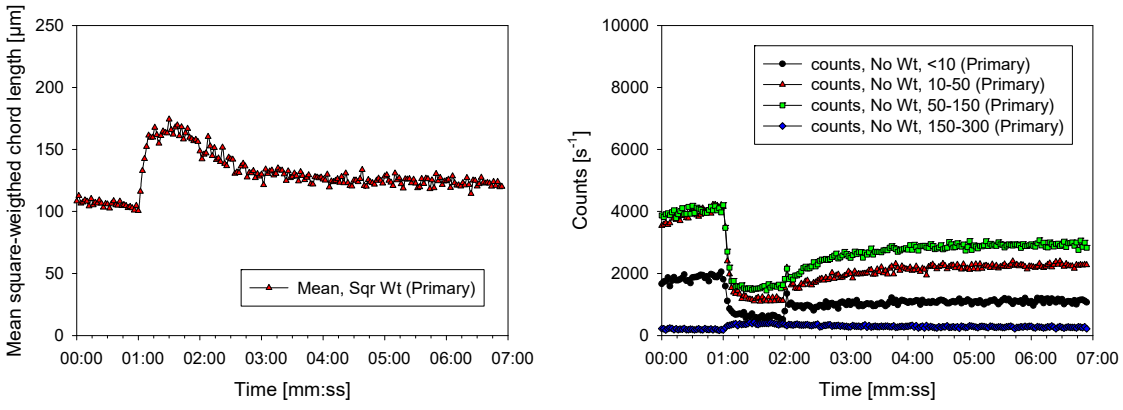

(**A**) (**B**)

Figure 8. (**A**) Mean square chord length and (**B**) counts evolution of suspension: 5 ppm of guar gum added after 1 min (MIBC 20 ppm, PAX 75 ppm).

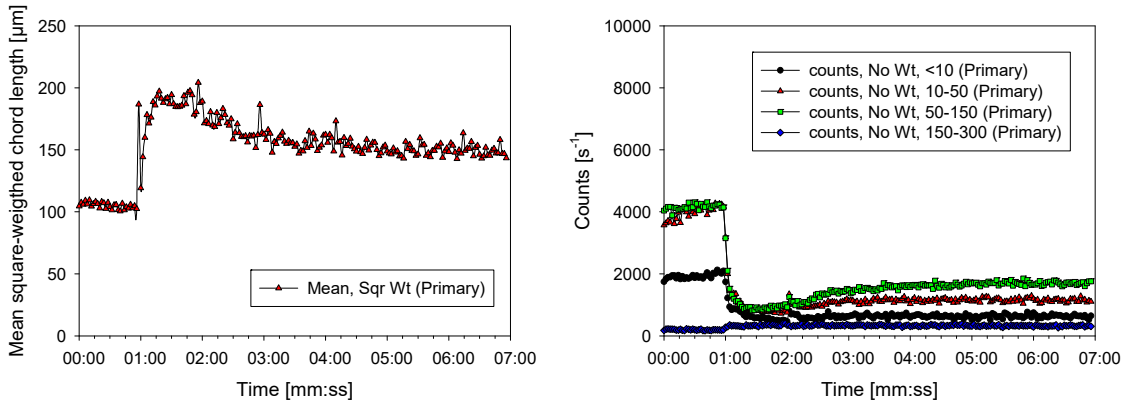

(**A**) (**B**)

Figure 9. (**A**) Mean square chord length and (**B**) counts evolution of suspension: 100 ppm of guar gum added after 1 min (MIBC 20 ppm, PAX 75 ppm).

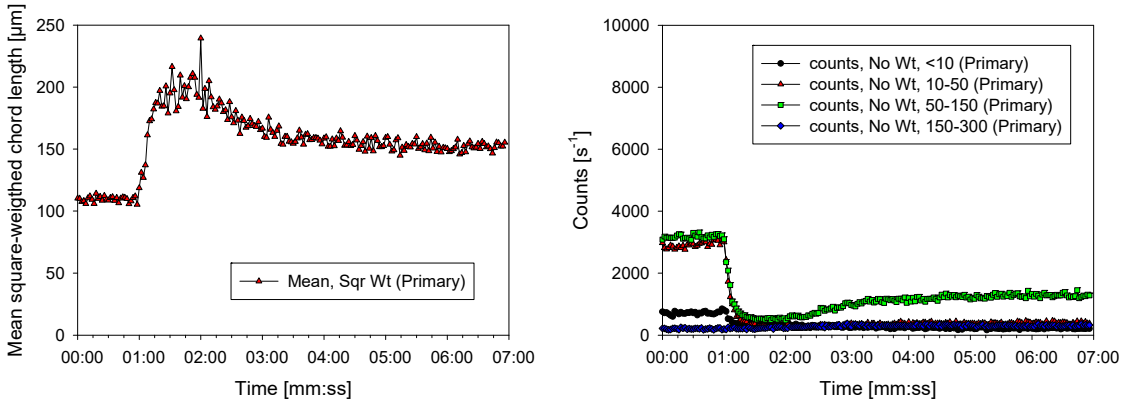

(**A**) (**B**)

Figure 10. (**A**) Mean square chord length and (**B**) counts evolution of suspension: 200 ppm of guar gum added after 1 min (MIBC 20 ppm, PAX 75 ppm).

Figures 11–13 present images of suspended pyrite particles and their conformation in the absence and presence of guar gum, PAX, and MIBC. In the absence of these reagents (Figure 11), the particles are mostly dispersed and a low number of agglomerates are noted. This was expected, as particles seek to agglomerate in a highly saline environment due to compression of the electrical double layer. The increasing formation of aggregates as the dose of guar gum increases is observed in Figure 12A for 5 ppm and in Figure 13A for 100 ppm. Although the shape of the aggregates is irregular and different from a sphere, it is seen that in both cases the floc structures are compact, and composed of several particles. After the addition of PAX and MIBC, particle redispersion is evident as depicted in Figure 12B (5 ppm), where the aggregates reduce their size but gain in sphericity. At 100 ppm guar gum (Figure 13B), there is no substantial reduction in the extent of the agglomerates. There is an apparent redistribution of the particles changing the shape of the floc structure; however, this is consistent with that reported above for the size of the flocs.

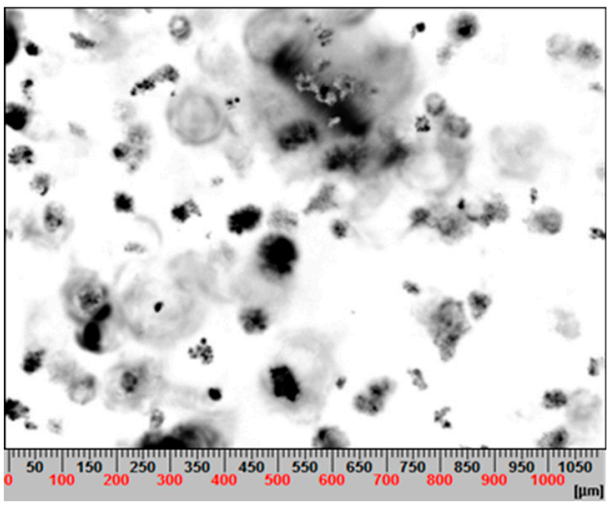

Figure 11. Suspended particles of pyrite in seawater at pH 8 (7 min).

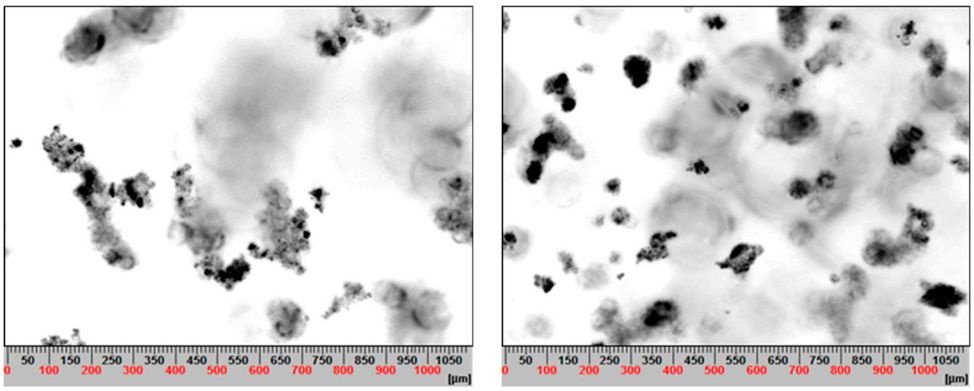

(**A**) (**B**)

Figure 12. Suspended particles of pyrite in seawater at pH 8 interacting with flotation reagents: (**A**) 5 ppm of guar gum (7 min) and (**B**) 5 ppm of guar gum, 75 ppm of PAX, and 20 ppm of MIBC (7 min).

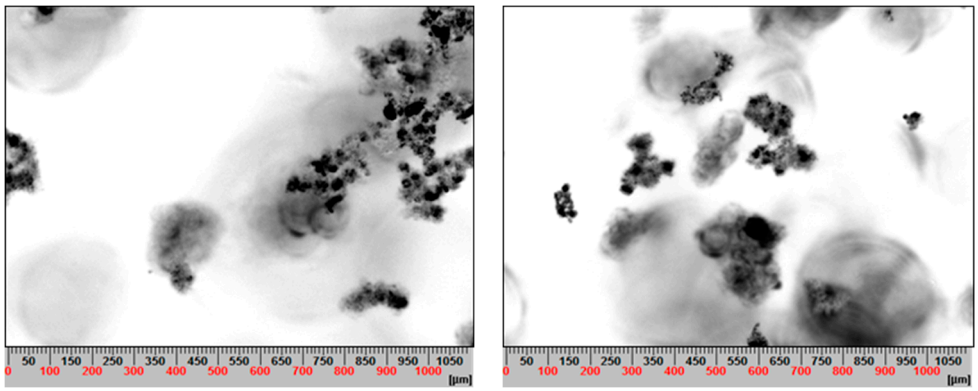

(A) **(B)**

Figure 13. Suspended particles of pyrite in seawater at pH 8 interacting with flotation reagents: (**A**) 100 ppm of guar gum (7 min) and (**B**) 100 ppm of guar gum, 75 ppm of PAX, and 20 ppm of MIBC (7 min).

3.3. FTIR Analysis

Figure 14 presents the spectra of guar gum, PAX, pyrite contacted with guar gum, and pyrite contacted with both PAX and guar gum in seawater at pH 8. The bands between 1700 and 3000 cm^{-1} and 1200 and 1500 cm^{-1} are due to the groups CH_2 and CH_3 of the collector alkyl (Figure 14A) [42]. The bands between 3000 and 3700 cm^{-1} are attributed to the hydrogen bonds of hydroxyl groups, due to hydroxides and oxy-hydroxide iron species [42]. The band at 3450 cm^{-1} is due to the stretching vibration of the hydroxyl groups in the guar gum structure. This indicates that hydrogen bonds strongly link to the O–H groups (Figure 14B).

In Figure 14C, the band at 1650 cm^{-1} is characteristic of water molecules indicating sulfate hydration [43]. The intense band at 1650 cm^{-1} suggests a stretch of the glucopyranose ring. This is indicative that the pyrite surface is more hydrated and hydrophilic. The bands between 900 and 1200 cm^{-1} corresponds to the asymmetric oxygen vibration (C-O-C), attributed to the xanthate and may be dixanthogen. The bands between 1000 and 1050 cm^{-1} are due to the vibration C=S [44]. Finally, the bands between 900 and 650 cm^{-1} correspond to oxidized iron species on pyrite such as the oxyhydroxides goethita (α-FeOOH) and limonite (α-$FeOOH{\cdot}nH_2O$)) [43]. Accordingly, it is confirmed that the pyrite surface is oxidized and this oxidation occurs rapidly. The bands in the ranges 1300 to 850 cm^{-1}, belong to sulfate species, such as iron sulfates ($Fe_2(SO_4)_3xH_2O$ between the bands 1000 and 1150 cm^{-1}).

The bands between 500 to 750 cm^{-1} are due to the stretching of the guar gum ring. As noted, they appeared in the guar gum–pyrite spectrum at 750 and 850 cm^{-1} (Figure 14D), indicating Guar Gum on the pyrite surface. In the guar gum–PAX–pyrite spectrum (Figure 14C), they are almost entirely reduced. This is an indication that PAX desorbed some Guar gum and co-adsorption of PAX and guar gum took place on the pyrite.

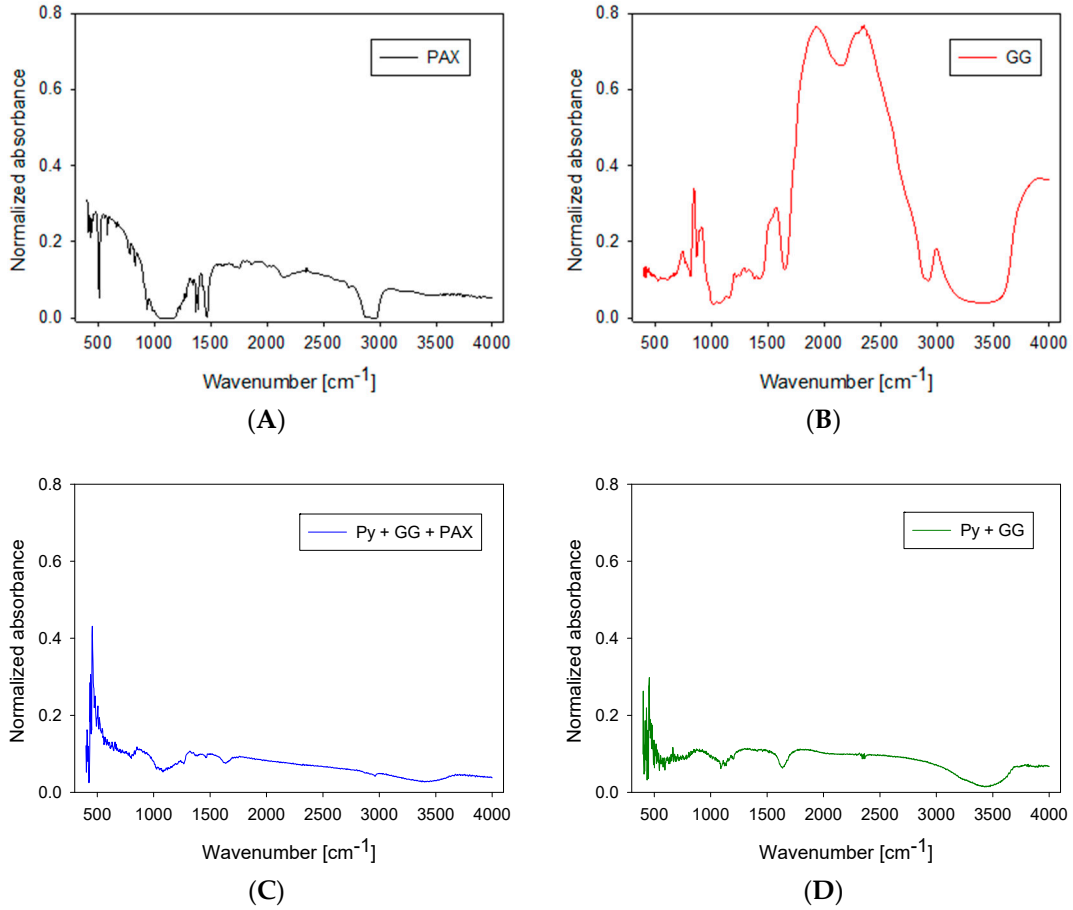

Figure 14. FTIR spectra for (**A**) PAX, (**B**) guar gum (GG), (**C**) pyrite (Py) + GG + PAX, and (**D**) Py + GG (pH 8, 35 ppm of PAX, 20 ppm of guar gum).

3.4. Surface Tension

Figure 15 shows the surface tension of seawater as a function of MIBC and guar gum concentrations. Both reagents affected the surface tension at low concentrations. At 5 ppm, the surface tension dropped by approximately 10%. In this study, a fixed concentration of MIBC (20 ppm) was used while varying the guar gum concentration from 0 to 200 ppm However, a synergistic effect in the surface tension is not noted by adding the two reagents. This result is not in agreement with others reported elsewhere stating that there is a synergistic effect when polymers are mixed with frothers [45,46]. The synergistic effect would cause an overstabilization of the bubbles, which would increase gangue mechanical entrainment lowering the concentrate quality. Accordingly, if guar gum were used in flotation it would not affect the bubbles characteristics so bubble overstabilization would be avoided.

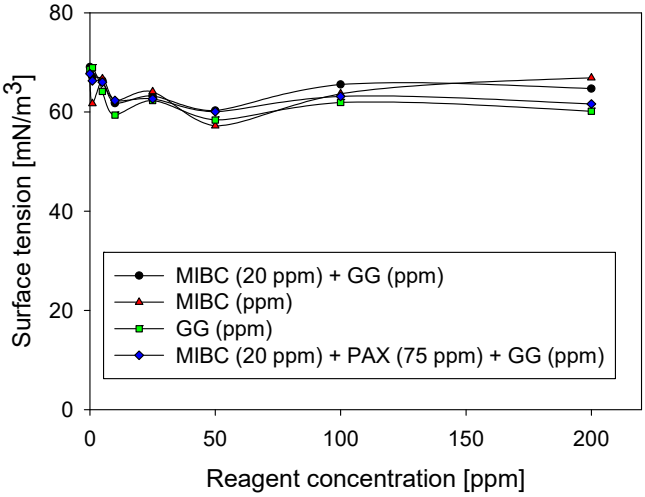

Figure 15. Surface tension as a function of reagents concentrations: (i) varied guar gum (GG) + 20 ppm of MIBC, (ii) varied MIBC, (iii) varied guar gum, and (iv) varied guar gum + 20 ppm of MIBC + 75 ppm of PAX (seawater at pH 8).

4. Discussion

Pyrite is common in cooper and polymetallic ore deposits. It is floatable and shows a high affinity with the flotation collectors that are used to concentrate the valuable metal sulfides. Therefore, flotation of pyrite is desirable as it impacts the quality of the metal concentrate.

Traditionally, pyrite is depressed at highly alkaline conditions. However, this approach cannot be implemented in seawater as precipitation of calcium and magnesium ions affects the performance of valuable minerals. Besides, there is an excessive consumption of lime, due to the buffer effects, that restricts the sustainability of depressing pH at high pH [15]. The current strategy operates at the slurry's natural pH and applies reagents that can selectively depress pyrite [47]. In this context, the organic reagents has shown promising results in the copper, molybdenum, talc, mica, galena, sphalerite, and pyrrhotite flotation [2]. However, their performance in seawater has not been explored yet, where a highly saline environment modifies the electrostatic interactions between surfaces and alters the structure in which water molecules are organized. It brings significant consequences in mineral processing.

Guar gum, used in this study, presented encouraging results, as FTIR studies indicate that this reagent was able to interact with the pyrite, decreasing its recovery from 80% to 23% in the presence of PAX. Although, the use of polysaccharides in general (guar gum, dextrin, starch, etc.) requires that the surface of pyrite should be oxidized at a certain level to achieve the interaction between the OH groups of the guar gum. The more ferric hydroxide on the pyrite surface, the higher is the adsorption of the polysaccharide [30].

The polysaccharide is expected to act by two mechanisms. On the one hand, the coating of the pyrite surface prevents the formation of $ROCS_2$-M bonds, which maintain the connection between the collector and the pyrite surface. Additionally, the in situ analysis of the particles employing the FBRM and PVM techniques revealed their flocculation. The hydrodynamic conditions exert stress that redisperses the particles, especially for low polymer dosages. At the same time, as the concentration of guar gum increases, the redispersing of the flocs decreases, due to the greater strength of the agglomerate structure. As the aggregates of pyrite are massive, even if the bubbles attach to them, the bubbles will not be able to transport them to the flotation froth so they will not float. Although the polymer is a surface active agent, the surface tension results indicate that there is not a synergistic effect with the frother, as has been reported elsewhere [46]. Overdose of guar gum saturate the surface of pyrite, limiting the size of the agglomerates. This leads to an increase in recovery as less massive aggregates formed, which can be carried to the froth phase by bubbles.

5. Conclusions

Guar gum was used to promote pyrite depression in flotations with seawater in the presence of the collector propyl xanthate. The tests were performed at natural pH to emulate the operating conditions of copper concentration plants using seawater. The results were promising, and it was found that the polysaccharide efficiently depressed pyrite in a highly saline environment. The polysaccharide adsorbs on the pyrite surface turning it very hydrophilic on top of the hydrophobicity due to adsorbe collector. The depression of pyrite was accompanied by strong flocculation of particles that generated massive aggregates, which are difficult to be transported by bubbles to the froth phase. However, the collector and frother (PAX and MIBC) redispersed the agglomerates making possible their levitation to the froth by bubbles. This can be reduced by increasing the polymer concentration to minimize the redispersion of the agglomerates. However, an overdose of guar gum leads to a re-stabilization of the agglomerates lowering its depression effect for the pyrite.

Author Contributions: The manuscript was written through the contributions of all authors. R.I.J. designed the research, C.I.C. and E.C.P. performed the experiments, C.I.C. wrote the first draft, R.I.J., P.R., N.T., and A.L.-V. analyzed the results and wrote the manuscript. All authors have read and agreed to the published version of the manuscript.

Funding: This research was funded by Conicyt Fondecyt 11171036 and Centro CRHIAM through Project ANID/FONDAP/15130015.

Acknowledgments: R.I.J. thanks CONICYT Fondecyt 11171036 and Centro de Recursos Hídricos para la Agricultura y la Minería (CRHIAM) through Project ANID/FONDAP/15130015. Pedro Robles thanks the Pontificia Universidad Católica de Valparaíso for the support provided.

Conflicts of Interest: The authors declare no conflicts of interest.

References

1. Wang, X.-H.; Eric Forssberg, K.S. Mechanisms of pyrite flotation with xanthates. *Int. J. Miner. Process.* **1991**, *33*, 275–290. [CrossRef]
2. Mu, Y.; Peng, Y.; Lauten, R.A. The depression of pyrite in selective flotation by different reagent systems—A Literature review. *Miner. Eng.* **2016**, *96–97*, 143–156. [CrossRef]
3. Boulton, A.; Fornasiero, D.; Ralston, J. Depression of iron sulphide flotation in zinc roughers. *Miner. Eng.* **2001**, *14*, 1067–1079. [CrossRef]
4. Jiang, C.L.; Wang, X.H.; Parekh, B.K.; Leonard, J.W. The surface and solution chemistry of pyrite flotation with xanthate in the presence of iron ions. *Colloids Surf. A* **1998**, *136*, 51–62. [CrossRef]
5. Trahar, W.J.; Senior, G.D.; Shannon, L.K. Interactions between sulphide minerals—The collectorless flotation of pyrite. *Int. J. Miner. Process.* **1994**, *40*, 287–321. [CrossRef]
6. Chandra, A.P.; Gerson, A.R. The mechanisms of pyrite oxidation and leaching: A fundamental perspective. *Surf. Sci. Rep.* **2010**, *65*, 293–315. [CrossRef]
7. Karthe, S.; Szargan, R.; Suoninen, E. Oxidation of pyrite surfaces: a photoelectron spectroscopic study. *Appl. Surf. Sci.* **1993**, *72*, 157–170. [CrossRef]
8. Moslemi, H.; Gharabaghi, M. A review on electrochemical behavior of pyrite in the froth flotation process. *J. Ind. Eng. Chem.* **2017**, *47*, 1–18. [CrossRef]
9. Hicyilmaz, C.; Emre Altun, N.; Ekmekci, Z.; Gokagac, G. Quantifying hydrophobicity of pyrite after copper activation and DTPI addition under electrochemically controlled conditions. *Miner. Eng.* **2004**, *17*, 879–890. [CrossRef]
10. Kocabag, D.; Shergold, H.L.; Kelsall, G.H. Natural oleophilicity/hydrophobicity of sulphide minerals, II. Pyrite. *Int. J. Miner. Process.* **1990**, *29*, 211–219. [CrossRef]
11. Zanin, M.; Lambert, H.; du Plessis, C.A. Lime use and functionality in sulphide mineral flotation: A review. *Miner. Eng.* **2019**, *143*, 105922. [CrossRef]
12. Li, Y.; Chen, J.; Kang, D.; Guo, J. Depression of pyrite in alkaline medium and its subsequent activation by copper. *Miner. Eng.* **2012**, *26*, 64–69. [CrossRef]
13. Cisternas, L.A.; Gálvez, E.D. The use of seawater in mining. *Miner. Process. Extr. Metall. Rev.* **2018**, *39*, 18–33. [CrossRef]

14. Jeldres, R.I.; Calisaya, D.; Cisternas, L.A. An improved flotation test method and pyrite depression by an organic reagent during flotation in seawater. *J. South. Afr. Inst. Min. Metall.* **2017**, *117*, 499–504. [CrossRef]
15. Castro, S. Challenges in flotation of Cu-Mo sulfide ores in sea water I. In *Water in Mineral Processing*; SME: Englewood, CO, USA, 2012; pp. 29–40.
16. Jeldres, R.I.; Arancibia-Bravo, M.P.; Reyes, A.; Aguirre, C.E.; Cortes, L.; Cisternas, L.A. The impact of seawater with calcium and magnesium removal for the flotation of copper-molybdenum sulphide ores. *Miner. Eng.* **2017**, *109*, 10–13. [CrossRef]
17. Li, W.; Li, Y.; Xiao, Q.; Wei, Z.; Song, S. The influencing mechanisms of sodium hexametaphosphate on chalcopyrite flotation in the presence of MgCl2 and CaCl2. *Minerals* **2018**, *8*, 150. [CrossRef]
18. Li, Y.; Li, W.; Xiao, Q.; He, N.; Ren, Z.; Lartey, C.; Gerson, A. The influence of common monovalent and divalent chlorides on chalcopyrite flotation. *Minerals* **2017**, *7*, 111. [CrossRef]
19. Suyantara, G.P.W.; Hirajima, T.; Miki, H.; Sasaki, K. Floatability of molybdenite and chalcopyrite in artificial seawater. *Miner. Eng.* **2018**, *115*, 117–130. [CrossRef]
20. Cao, Z.; Chen, X.; Peng, Y. The role of sodium sulfide in the flotation of pyrite depressed in chalcopyrite flotation. *Miner. Eng.* **2018**, *119*, 93–98. [CrossRef]
21. Göktepe, F. Effect of H2O2 and NaSH addition to change the electrochemical potential in flotation of chalcopyrite and pyrite minerals. *Miner. Process. Extr. Metall. Rev.* **2010**, *32*, 24–29. [CrossRef]
22. Hassanzadeh, A.; Hasanzadeh, M. Chalcopyrite and pyrite floatabilities in the presence of sodium sulfide and sodium metabisulfite in a high pyritic copper complex ore. *J. Dispers. Sci. Technol.* **2017**, *38*, 782–788. [CrossRef]
23. Khmeleva, T.N.; Skinner, W.; Beattie, D.A.; Georgiev, T.V. The effect of sulphite on the xanthate-induced flotation of copper-activated pyrite. *Physicochem. Prob. Miner. Process.* **2002**, *36*, 185–195.
24. Kar, B.; Sahoo, H.; Rath, S.S.; Das, B. Investigations on different starches as depressants for iron ore flotation. *Miner. Eng.* **2013**, *49*, 1–6. [CrossRef]
25. Lopez Valdivieso, A.; Sánchez López, A.A.; Song, S.; García Martínez, H.A.; Licón Almada, S. Dextrin as a regulator for the selective flotation of chalcopyrite, galena and pyrite. *Can. Metall. Q.* **2007**, *46*, 301–309. [CrossRef]
26. Wang, Z.; Xie, X.; Xiao, S.; Liu, J. Adsorption behavior of glucose on pyrite surface investigated by TG, FTIR and XRD analyses. *Hydrometallurgy* **2010**, *102*, 87–90. [CrossRef]
27. Sarquís, P.E.; Menéndez-Aguado, J.M.; Mahamud, M.M.; Dzioba, R. Tannins: the organic depressants alternative in selective flotation of sulfides. *J. Clean. Prod.* **2014**, *84*, 723–726. [CrossRef]
28. Rutledge, J.; Anderson, C. Tannins in mineral processing and extractive metallurgy. *Metals* **2015**, *5*, 1520–1542. [CrossRef]
29. Mu, Y.; Peng, Y.; Lauten, R.A. Electrochemistry aspects of pyrite in the presence of potassium amyl xanthate and a lignosulfonate-based biopolymer depressant. *Electrochim. Acta* **2015**, *174*, 133–142. [CrossRef]
30. Lopez-Valdivieso, A.; Sanchez-López, A.A.; Padilla-Ortega, E.; Robledo-Cabrera, A.; Galvez, E.; Cisternas, L.A. Pyrite depression by dextrin in flotation with xanthates. Adsorption and floatability studies. *Physicochem. Prob. Miner. Process.* **2018**, *54*, 1159–1171. [CrossRef]
31. Mathur, N.K. *Industrial Galactomannan Polysaccharides*; CRC Press: Boca Raton, FL, USA, 2016; ISBN 9780429105142.
32. Laskowski, J.S.; Liu, Q.; O'Connor, C.T. Current understanding of the mechanism of polysaccharide adsorption at the mineral/aqueous solution interface. *Int. J. Miner. Process.* **2007**, *84*, 59–68. [CrossRef]
33. Ma, X.; Pawlik, M. Adsorption of guar gum onto quartz from dilute mixed electrolyte solutions. *J. Colloid Interface Sci.* **2006**, *298*, 609–614. [CrossRef] [PubMed]
34. Ma, X.; Pawlik, M. Role of background ions in guar gum adsorption on oxide minerals and kaolinite. *J. Colloid Interface Sci.* **2007**, *313*, 440–448. [CrossRef] [PubMed]
35. Mailula, T.D.; Bradshaw, D.J.; Harris, P.J. The effect of copper sulphate addition on the recovery of chromite in the flotation of UG2 ore. *J. S. Afr. Inst. Min. Metall.* **2003**, *103*.
36. Shortridge, P.; Harris, P.; Bradshaw, D.; Koopal, L. The effect of chemical composition and molecular weight of polysaccharide depressants on the flotation of talc. *Int. J. Miner. Process.* **2000**, *59*, 215–224. [CrossRef]
37. Bicak, O.; Ekmekci, Z.; Bradshaw, D.J.; Harris, P.J. Adsorption of guar gum and CMC on pyrite. *Miner. Eng.* **2007**, *20*, 996–1002. [CrossRef]

38. Jeldres, M.; Piceros, E.C.; Toro, N.; Torres, D.; Robles, P.; Leiva, W.H.; Jeldres, R.I. Copper tailing flocculation in seawater: Relating the yield stress with fractal aggregates at varied mixing conditions. *Metals* **2019**, *9*, 1295. [CrossRef]
39. Hu, Y.; Sun, W.; Wang, D. *Electrochemistry of Flotation of Sulphide Minerals*; Springer: Berlin/Heidelberg, Germany, 2009; ISBN 978-3-540-92178-3.
40. López Valdivieso, A.; Sánchez López, A.A.; Song, S. On the cathodic reaction coupled with the oxidation of xanthates at the pyrite/aqueous solution interface. *Int. J. Miner. Process.* **2005**, *77*, 154–164. [CrossRef]
41. López Valdivieso, A.; Celedón Cervantes, T.; Song, S.; Robledo Cabrera, A.; Laskowski, J. Dextrin as a non-toxic depressant for pyrite in flotation with xanthates as collector. *Miner. Eng.* **2004**, *17*, 1001–1006. [CrossRef]
42. Rath, R.K.; Subramanian, S.; Pradeep, T. Surface chemical studies on pyrite in the presence of polysaccharide-based flotation depressants. *J. Colloid Interface Sci.* **2000**, *229*, 82–91. [CrossRef]
43. Kongolo, M.; Benzaazoua, M.; de Donato, P.; Drouet, B.; Barrès, O. The comparison between amine thioacetate and amyl xanthate collector performances for pyrite flotation and its application to tailings desulphurization. *Miner. Eng.* **2004**, *17*, 505–515. [CrossRef]
44. Leppinen, J.O. FTIR and flotation investigation of the adsorption of ethyl xanthate on activated and non-activated sulfide minerals. *Int. J. Miner. Process.* **1990**, *30*, 245–263. [CrossRef]
45. Tan, S.N.; Pugh, R.J.; Fornasiero, D.; Sedev, R.; Ralston, J. Foaming of polypropylene glycols and glycol/MIBC mixtures. *Miner. Eng.* **2005**, *18*, 179–188. [CrossRef]
46. Wang, Y.; Lauten, R.A.; Peng, Y. The effect of biopolymer dispersants on copper flotation in the presence of kaolinite. *Miner. Eng.* **2016**, *96–97*, 123–129. [CrossRef]
47. Ramos, O.; Castro, S.; Laskowski, J.S. Copper–molybdenum ores flotation in sea water: Floatability and frothability. *Miner. Eng.* **2013**, *53*, 108–112. [CrossRef]